Net Atmospheric Mercury Deposition to Svalbard: Estimates from Lacustrine Sediments

Paul E. Drevnick[a*], Handong Yang[b], Carl H. Lamborg[c], and Neil L. Rose[b]

[a]INRS-ETE, Université du Québec, 490 de la Couronne, Québec, QC G1K 9A9, Canada, [b]Environmental Change Research Centre, University College London, Gower Street, London WC1E 6BT, United Kingdom, [c]Deparment of Marine Chemistry & Geochemistry, Woods Hole Oceanographic Institution, Woods Hole, MA 02543, USA

[*]Corresponding author: paul.drevnick@ete.inrs.ca; Tel. +1 418 654 2519; Fax +1 418 654 2600

Abstract

In this study we used lake sediments, which faithfully record Hg inputs, to derive estimates of net atmospheric Hg deposition to Svalbard, Norwegian Arctic. With the exception of one site affected by local pollution, the study lakes show twofold to fivefold increases in sedimentary Hg accumulation since 1850, likely due to long-range atmospheric transport and deposition of anthropogenic Hg. Sedimentary Hg accumulation in these lakes is a linear function of the ratio of catchment area to lake area, and we used this relationship to model net atmospheric Hg flux: preindustrial and modern estimates are 2.5±3.3 μg/m^2/y and 7.0±3.0 μg/m^2/y, respectively. The modern estimate, by comparison with data for Hg wet deposition, indicates that atmospheric mercury depletion events (AMDEs) or other dry deposition processes contribute approximately half (range 0-70%) of the net flux. Hg from AMDEs may be moving in significant quantities into aquatic ecosystems, where it is a concern because of contamination of aquatic food webs.

Keywords: mercury, atmospheric deposition, Arctic, Svalbard, lake sediments

1. Introduction

Mercury (Hg) is released to the atmosphere by human activities, mostly in temperate regions, and is transported by prevailing winds to the Arctic (AMAP/UNEP, 2008). The net deposition of Hg from the atmosphere to sensitive arctic ecosystems is poorly characterized (Durnford and Dastoor, 2011), but is sufficient to result in high concentrations of this toxic metal in aquatic food webs (Poissant et al., 2008). Hg contamination of traditional food sources (e.g., fish, seals, whales) poses a serious health risk to arctic peoples (Donaldson et al., 2010).

Uncertainty over net depositional fluxes of Hg to arctic ecosystems stems from the discovery by Schroeder et al. (1998) of atmospheric mercury depletion events (AMDEs), in which nearly all Hg in the lower troposphere is oxidized and deposited in a period of days to weeks during polar sunrise. Rapid removal of Hg from the troposphere is the result of complex atmospheric chemistry, likely involving reactive halogen species (Ariya et al., 2002; Holmes et al., 2010). Lindberg et al. (2002) suggested that AMDEs may be a recent phenomenon due to increased production of reactive halogens from an Arctic Ocean increasingly free of multi-year ice. This hypothesis is supported by the recent observations of Nghiem et al. (2012) that AMDEs are coupled to bromine (halogen) "explosions" from seasonal ice, which is saltier than the multi-year ice it has replaced. Fluxes of Hg associated with AMDEs have been estimated to be 2.5-10 μg/m^2/y (Skov et al., 2004), but it is thought that much of what is deposited is rapidly

photoreduced in the snowpack and returned to the atmosphere (Lalonde et al., 2003; Sherman et al., 2010). Constraining Hg fluxes from windblown and melting snow can be exceedingly difficult. In this study, we instead used lake sediments, which are reliable archives of Hg accumulation (Biester et al., 2007), to derive estimates of net atmospheric Hg flux to arctic ecosystems – in this case to Svalbard (Norwegian Arctic).

2. Methods

^{210}Pb-dated sediment cores from 5 lakes in Svalbard were analyzed for total Hg. The lakes, located along the west coast of the main island of Spitsbergen, include Ossian Sarsfjellet (C), Ytertjørna (Q), Vassauga (S), Daltjørna (T), and Tendammen (U). Details of the lakes, as well as the collection, processing, and dating of cores can be found in Appleby (2004) and Birks et al. (2004b). A suite of biostratigraphical and geochemical analyses (though not Hg) were previously performed on these cores, and the results are summarized in Birks et al. (2004a). Total Hg was analyzed by thermal combustion with a DMA-80 Direct Mercury Analyzer or acid digestion followed by cold vapor atomic absorption spectrometry. Methods, including quality assurance procedures, followed previous reports (Drevnick et al., 2010; Yang et al., 2002). Accumulation rates of Hg in sediment were calculated by multiplying ^{210}Pb-based sedimentation rates by Hg concentrations. Hg accumulation rates were not corrected for sediment focusing, because Appleby (2004) determined that "focusing is not a major factor at these sites".

To derive net atmospheric Hg fluxes we used the approach of Swain et al. (1992), which involves simple linear regression of sedimentary Hg accumulation (dependent variable) and the catchment area to lake area ratio (A_C:A_L; independent variable). The intercept of the regression line represents net atmospheric Hg flux to a lake with no catchment, i.e. wet and dry deposition minus evasion and outflow. The slope represents the additional flux of Hg delivered from catchment to lake for each unit increase in A_C:A_L. Assuming all Hg in the catchment comes from the atmosphere (for our study lakes, other sources are likely insignificant), the ratio of slope to intercept represents the proportion of Hg deposited to the catchment that is transported to the lake.

3. Results and Discussion

Hg concentrations and Hg accumulation rates in sediments increase from relatively low values in preindustrial sediments to peak values in recent sediments (Fig. 1). Four of the lakes (C, Q, S, T) show similar magnitudes of change. Concentrations increase up-core from 20-50 ng/g dry wt to 60-90 ng/g dry wt, and accumulation rates, with the change expressed as accumulation ratios (Fig. 2), increase twofold to fivefold from preindustrial to recent sediments. These results are consistent with other studies of lake sediments throughout the Arctic (e.g., Bindler et al., 2001; Fitzgerald et al., 2005; Hermanson, 1998; Jiang et al., 2011; Landers et al., 1998; Lockhart et al, 1995 and 1998; Muir et al., 2009), as well as outside of the Arctic (see recent summary in Table 1 of Yang et al., 2010), that concluded recent increases are due to long-range atmospheric transport and deposition of anthropogenic Hg. The fifth lake, Tendammen (U), has recent sediments that are more contaminated with Hg than the other lakes. In this lake, sediments deposited since 1970 have concentrations greater than 100 ng/g dry wt and accumulation ratios of 10-20. These high values indicate Tendammen (U) is affected by a local pollution source, likely the coal-fired power station at the nearby community of Longyearbyen (Rose et al., 2004).

Among the study lakes, sedimentary Hg accumulation is a linear function of A_C:A_L (Fig. 3), validating the use of the model by Swain et al. (1992) to derive net atmospheric Hg fluxes. The regression equations are preindustrial Hg = 2.5±3.3 + 0.13±0.06 x A_C:A_L (r^2 = 0.655, p = 0.196, n = 4) and modern Hg = 7.0±3.0 + 0.26±0.06 x A_C:A_L (r^2 = 0.911, p = 0.046, n = 4) (error terms represent SE). Intercept and slope estimates indicate net atmospheric Hg flux and flux from catchment to lake have increased twofold to threefold from preindustrial to modern times. Ratios of slope to intercept for the preindustrial and modern regression equations indicate the proportion of Hg deposited to the catchment that is transported to the lake is 4-5% and has changed little with time.

Because of a lack of local or regional data for which to directly compare our estimate for preindustrial net atmospheric Hg flux, it is difficult to determine whether AMDEs had an effect on net flux (or even occurred) before the industrial period. However, the observation that the degree of industrial enhancement (twofold to fivefold increase in sedimentary Hg accumulation) is comparable to other pristine regions of the globe suggests that whatever processes are currently in effect in Svalbard today were likely occurring in the preindustrial past. If this were not true, we should have observed a larger enhancement in Hg accumulation.

Comparison of our estimate of modern net atmospheric Hg flux (7.0±3.0 μg/m^2/y) with independent estimates of Hg wet deposition provides support for AMDEs or other dry deposition processes presently contributing a significant portion of net flux. Berg et al. (2001) measured total Hg in samples from rain events in 1996-1997 and reported an average (± SE) concentration of 14.2±4.0 ng/L, which suggests an annual flux from wet deposition of 4.3±1.3 μg/m^2/y. This estimate requires that total Hg concentrations in rain and snow are similar, which given the values reported by Ferrari et al. (2005) for fresh snow (mean ± SE; 11.0±2.1 ng/L during AMDEs, 10.4±1.5 ng/L during non-AMDE periods) appears accurate. Lamborg et al. (2000) found a linear relationship between Hg and ^{210}Pb in precipitation at a site in northern Wisconsin (USA), and developed an equation to predict contemporary Hg wet deposition from ^{210}Pb: Hg flux = ^{210}Pb flux x 0.06±0.01 μg/Bq + rain depth x 2±2 μg/m^3. The relationship has been verified at a site in arctic Alaska (Fitzgerald et al. 2005). ^{210}Pb flux and rain depth for Spitsbergen are approximately 56 Bq/m^2/y (Appleby 2004) and 0.3 m/y (Norwegian Meteorological Institute 2012), respectively, amounting to Hg wet deposition of 3.96±1.16 μg/m^2/y. Thus, Hg wet deposition appears to be about 4 μg/m^2/y. Our estimate represents (per the model of Swain et al., 1992, and stated above) net atmospheric Hg flux to a lake with no catchment, i.e. wet deposition plus dry deposition minus evasion minus outflow. To calculate the minimum contribution of dry deposition to net atmospheric flux, the loss terms (evasion, outflow) can be cancelled out, reducing the equation to net atmospheric flux (7.0±3.0 μg/m^2/y) equals wet deposition (4.0±1.0 μg/m^2/y) plus dry deposition. Dry deposition then equals 3.0±4.0 μg/m^2/y, or 43% (range 0-70%) of the net flux. Evasion and outflow can be significant loss terms in Hg budgets for arctic lakes, however. In seepage lakes in arctic Alaska, evasion constituted 22-45% of inputs (Fitzgerald et al., 2005). In the Canadian Arctic, 59% of Hg inputs to a drainage lake were discharged through the outflow (Semkin et al., 2005). If either of these sinks are significant in our study lakes (all of which are drainage lakes), a larger contribution from dry deposition would be required to account for the losses.

AMDEs are likely the dominant process for dry deposition of Hg to Svalbard. AMDEs have been documented at Svalbard (Berg et al., 2003) and are associated with a large downward flux of Hg. Skov et al. (2004) used the Danish Eulerian Hemispheric Model to estimate a flux from AMDEs of 6 μg/m^2/y (at Svalbard). This value agrees well with empirical data from

Dommergue et al. (2010). During spring of 2007 at Ny-Ålesund, nine AMDEs were recorded: two "long" events (each with a flux of 0.72-2.16 μg/m^2) and seven "short and shallow" events (each with a flux of 0.2-0.65 μg/m^2). Combined, the events add up to a total flux of 2.84-8.87 μg/m^2/y.

In contrast to AMDEs, other dry deposition processes are likely insignificant, except perhaps at our impacted site (U). In urban environments and near point sources, dry deposition of Hg associated with particulate matter can be significant (Keeler et al., 1995). This process could be important at Tendammen (U), which is near a coal-fired power station, but (because it is impacted by a point source) we did not include this lake in the model for our modern estimate of net flux. In areas of the Arctic not impacted by point sources (including our four other study lakes), concentrations of particulate Hg are low (confirmed at Ny-Ålesund by Steen et al., 2011), and thus dry deposition of particulate Hg is likely insignificant. For example, Fitzgerald et al. (2005) reported for lakes in arctic Alaska a dry depositional flux from particulate Hg of 0.1 μg/m^2/y. Dry deposition of Hg can also include uptake of Hg by terrestrial plants. Elevated Hg concentrations in vegetation at coastal sites compared to inland sites of the Arctic have been reported (Berg et al. 2008, Carignan and Sonke 2010, Landers et al. 1995). Carignan and Sonke (2010) used correlations between Hg and halogens (in the vegetation) to indicate that the Hg is due to AMDEs. Terrestrial vegetation is unlikely to be a conduit of atmospheric Hg to our study lakes, however, as the lakes' catchments consist of bare ground or sparse vegetation (Birks et al., 2004b).

4. Conclusions

Lake sediments from Svalbard show a twofold to fivefold increase in Hg accumulation since 1850. This increase, similar in magnitude to other regions of the globe, suggests that atmospheric processes (i.e., AMDEs) occurring at Svalbard today likely also occurred in the past. Further, by comparison with data for Hg wet deposition, our estimate for modern net atmospheric Hg flux indicates that AMDEs now contribute 43% (range 0-70%) of the net flux. A mass balance study, such as that conducted by Fitzgerald et al. (2005) for lakes in arctic Alaska, would better constrain inputs/losses of Hg to/from Svalbard lakes. From our study, however, it appears that Hg from AMDEs may be moving in significant quantities into aquatic ecosystems, where it is a concern because of contamination of aquatic food webs, including in Svalbard (Jaeger et al., 2009; Rognerud et al., 2002).

Acknowledgements

Funding was provided by an NSERC Discovery Grant (Drevnick) and the Norges forskningsråd (grant number 107745/730). Peter Appleby provided useful comments on an earlier draft.

Supplementary Data

All original data.

References

AMAP/UNEP, 2008. Technical Background Report to the Global Atmospheric Mercury Background Assessment. Arctic Monitoring and Assessment Programme, Oslo, Norway; UNEP Chemicals Branch, Geneva, Switzerland.

Appleby P.G. 2004. Environmental change and atmospheric contamination on Svalbard: sediment chronology. Journal of Paleolimnology 31, 433-443.

Ariya P.A., Khalizov A., Gidas A. 2002. Reactions of gaseous mercury with atomic and molecular halogens: kinetics, product studies, and atmospheric implications. Journal of Physical Chemistry A 106, 7310-7320.

Berg T., Aspmo K., Steinnes E. 2008. Transport of Hg from atmospheric mercury depletion events to the mainland of Norway and its possible influence on Hg deposition. Geophysical Research Letters 35, L09802, doi:10.1029/2008GL033586.

Berg T., Bartnicki J., Munthe J., Lattila H., Hrehoruk J., Mazur A. 2001. Atmospheric mercury species in the European Arctic: measurements and modeling. Atmospheric Environment 235, 2569-2582.

Berg T., Sekkesaeter S., Steinnes E., Valdal A.-K., Wibetoe G. 2003. Springtime depletion of mercury in the European Arctic as observed at Svalbard. Science of the Total Environment 304, 43-51.

Biester H., Bindler R., Martinez-Cortizas A., Engstrom D.R. 2007. Modeling the past atmospheric deposition of mercury using natural archives. Environmental Science & Technology 41, 4851-4860.

Bindler R., Renberg I., Appleby P.G., Anderson N.J., Rose N.L. 2001. Mercury accumulation rates and spatial patterns in lake sediments from west Greenland: a coast to ice margin transect. Environmental Science & Technology 35, 1736-1741.

Birks H.J.B., Jones V.J., Rose N.L. 2004a. Recent environmental change and atmospheric contamination on Svalbard as recorded in recent sediments – syntheses and general conclusions. Journal of Paleolimnology 31, 531-546.

Birks H.J.B., Monteith D.T., Rose N.L., Jones V.J., Peglar S.M. 2004b. Recent environmental change and atmospheric contamination on Svalbard as recorded in lake sediments – modern limnology, vegetation, and pollen deposition. Journal of Paleolimnology 31, 411-431.

Carignan J., Sonke J. 2010. The effect of atmospheric mercury depletion events on the net deposition flux around Hudson Bay, Canada. Atmospheric Environment 44, 4372-4379.

Dommergue A., Larose C., Faïn X., Clarisse O., Foucher D., Hintelmann H., Schneider D., Ferrari C.P. 2010. Deposition of mercury species in the Ny-Ålesund Area (79ºN) and their transfer during snowmelt. Environmental Science & Technology 44, 901-907.

Donaldson S.G., Van Oostdam J., Tikhonov C., Feeley M., Armstrong B., Ayotte P., Boucher O., Bowers W., Chan L., Dallaire F., Dallaire R., Dewailly É., Edwards J., Egeland G.M., Fontaine J., Furgal C., Leech T., Loring E., Muckle G., Nancarrow T., Pereg D., Plusquellec P., Potyrala M., Receveur O., Shearer R.G. 2010. Environmental contaminants and human health in the Canadian Arctic. Science of the Total Environment 408, 5165-5234.

Durnford D., Dastoor A. 2011. The behavior of mercury in the cryosphere: a review of what we know from observations. Journal of Geophysical Research 116, D06305, doi:10.1029/2010JD014809.

Drevnick P.E., Shinneman A.L.C., Lamborg C.H., Engstrom D.R., Bothner M.H., Oris J.T. 2010. Mercury flux to sediments of Lake Tahoe, California-Nevada. Water, Air, & Soil Pollution 210, 399-407.

Ferrari C.P., Gauchard P.-A., Aspmo K., Dommergue A., Magand O., Bahlmann E., Nagorski S, Temme C., Ebinghaus R., Steffen A., Banic C., Berg T., Planchon R., Barbante C., Cescon P., Boutron C.F. 2005. Atmospheric Environment 39, 7633-7645.

Fitzgerald W.F., Engstrom D.R., Lamborg C.H., Tseng C.-M., Balcom P.H., Hammerschmidt C.R. 2005. Modern and historic atmospheric mercury fluxes in northern Alaska: global sources and Arctic depletion. Environmental Science & Technology 39, 557-568.

Hermanson M.H. 1998. Anthropogenic mercury deposition to Arctic lake sediments. Water, Air, & Soil Pollution 101, 309-321.

Holmes C.D., Jacob D. J., Corbitt E.S., Mao J., Yang X., Talbot R., Slemr F. 2010. Global atmospheric model for mercury including oxidation by bromine atoms. Atmospheric Chemistry and Physics Discussions 10, 19845-19900.

Jaeger I., Hop H., Gabrielsen G.W. 2009. Biomagnification of mercury in selected species from an Arctic marine food web in Svalbard. Science of the Total Environment 407, 4744-4751.

Jiang S., Liu X., Chen Q. 2011. Distribution of total mercury and methylmercury in lake sediments in Arctic Ny-Ålesund. Chemosphere 83, 1108-1116.

Keeler G., Glinsorn G., Pirrone N. 1995. Particulate mercury in the atmosphere: its significance, transport, transformation, and sources. Water, Air, & Soil Pollution 80, 159-168.

Lalonde J.D., Amyot M. Doyon M.-R., Auclair J.-C. 2003. Photo-induced Hg(II) reduction in snow from the remote and temperate Experimental Lakes Area (Ontario, Canada). Journal of Geophysical Research 108(D6), 4200, doi:10.1029/2001JD001534.

Lamborg C.H., Fitzgerald W.F., Graustein W.C., Turekian K.K. 2000. An examination of the atmospheric chemistry of mercury using ^{210}Pb and ^{7}Be. Journal of Atmospheric Chemistry 36, 325-338.

Landers D.H., Ford J., Gubala C., Monetti M., Lasarsa B.K., Martinson J. 1995. Mercury in vegetation and lake sediments from the U.S. Arctic. Water, Air, & Soil Pollution 80, 591-601.

Landers D.H., Gubala C., Verta M., Lucotte M., Johansson K., Vlasova T., Lockhart W.L. 1998. Using lake sediment mercury flux ratios to evaluate the regional and continental dimensions of mercury deposition in Arctic and boreal ecosystems. Atmospheric Environment 32, 919-928.

Lindberg S.E., Brooks S., Lin C.-J. Scott K.J., Landis M.S., Stevens R.K., Goodsite M., Richter A. 2002. Dynamic oxidation of gaseous mercury in the Arctic troposphere at polar sunrise. Environmental Science & Technology 36, 1245-1256.

Lockhart W.L., Wilkinson P., Billeck B.N., Canell R.A., Hunt R.V., Brunskill G.J., Delaronde J., St. Louis V. 1998. Fluxes of mercury to lake sediments in central and northern Canada inferred from dated sediment cores. Biogeochemistry 40, 163-173.

Lockhart W.L., Wilkinson P., Billeck B.N., Hunt R.V., Wagemann R., Brunskill G.J. 1995. Current and historical inputs of mercury to high-latitude lakes in Canada and to Hudson Bay. Water, Air, & Soil Pollution 80, 603-610.

Muir D.C.G., Wang X., Yang F., Nguyen N., Jackson T.A., Evans M.S., Douglas M., Köck G., Lamoureux S., Pienitz R., Smol J.P., Vincent W.F., Dastoor A. 2009. Spatial trends and historical deposition of mercury in eastern and northern Canada inferred from lake sediment cores. Environmental Science & Technology 43, 4802-4809.

Nghiem S.V., Rigor I.G., Richter A., Burrows J.P., Shepson P. B., Bottenheim J., Barber D.G., Steffen A., Latonas J., Wang F., Stern G., Clemente-Colón P., Martin S., Hall D.K., Kaleschke L., Tackett P., Neumann G., Asplin M.G. 2012. Field and satellite observations of the formation and distribution of Arctic atmospheric bromine above a rejuvenated sea ice cover. Journal of Geophysical Research 117, D00S05, doi:10.1029/2011JD016268.

Norwegian Meteorological Institute. 2012. <http://met.no/English/>. Accessed 20 Mar. 2012.

Poissant L., Zhang H.H., Canário J., Constant P. 2008. Critical review of mercury fates and contamination in the Arctic tundra ecosystem. Science of the Total Environment 400, 173-211.

Rognerud S., Grimalt J.O., Rosseland B.O., Fernandez P., Hofer R., Lackner R., Lauritzen B., Lien L., Massabuau J.C., Ribes A. 2002. Mercury and organochlorine contamination in brown trout (*Salmo trutta*) and Arctic charr (*Salvelinus alpinus*) from high mountain lakes in Europe and the Svalbard archipelago. Water, Air, & Soil Pollution Focus 2, 209-232.

Rose N.L., Rose C.L., Boyle J.F., Appleby P.G. 2004. Lake-sediment evidence for local and remote sources of atmospherically deposited pollutants on Svalbard. Journal of Paleolimnology 31, 499-513.

Schroeder W.F., Anlauf K.G., Barrie L.A., Lu J.Y., Steffen A., Schneeberger D.R., Berg T. 1998. Arctic springtime depletion of mercury. Nature 394, 331-332.

Semkin R.G., Mierle G., Neureuther R.J. 2005. Hydrochemistry and mercury cycling in a High Arctic watershed. Science of the Total Environment 342, 199-221.

Sherman L.S., Blum J.D., Johnson K.P., Keeler G.J., Barres J.A., Douglas T.A. 2010. Mass-independent fractionation of mercury isotopes in Arctic snow driven by sunlight. Nature Geoscience 3, 173-177.

Skov H., Christensen J.H., Goodsite M.E., Heidam N.Z., Jensen B., Wåhlin P., Geernaert G. 2004. Fate of elemental mercury in the Arctic during atmospheric mercury depletion episodes and the load of atmospheric mercury to the Arctic. Environmental Science & Technology 38, 2373-2382.

Steen A.O., Berg T., Dastoor A.P., Durnford D.A., Engelsen O., Hole L.R., Pfaffhuber K.A. 2011. Natural and anthropogenic atmospheric mercury in the European Arctic: a fractionation study. Atmospheric Chemistry and Physics 11, 6273-6284.

Swain E.B., Engstrom D.R., Brigham M.E., Henning T.A., Brezonik P.L. 1992. Increasing rates of atmospheric mercury deposition in midcontinental North America. Science 257, 784-787.

Yang H., Engstrom D.R., Rose N.L. 2010. Recent changes in atmospheric mercury deposition recorded in the sediments of remote equatorial lakes in the Rwenzori Mountains, Uganda. Environmental Science & Technology 44, 6570-6575.

Yang H., Rose N.L., Battarbee R.W. 2002. Mercury and lead budgets for Lochnagar, a Scottish mountain lake and its catchment. Environmental Science & Technology 36, 1383-1388.

306 Figure Captions
307
308 Figure 1. ^{210}Pb age versus Hg concentration (gray symbols, lines) and Hg accumulation (black
309 symbols, lines) in sediment cores collected during 1995 from 5 lakes along the west coast of
310 Spitsbergen, Svalbard Archipelago, Norwegian Arctic. For Ossian Sarsfjellet (C), the Hg record
311 prior to *c.* 1918 is not reliable because of an episode of accelerated sedimentation (possibly a
312 "slump" event; Appleby 2004). For all other lakes, Hg records extend to preindustrial (pre-1850)
313 sediments. Age models were extrapolated below the base of the ^{210}Pb record by Appleby (2004).
314 Map is reprinted from Figure 1 of Journal of Paleolimnology, Vol. 31, 2004, pp.433-443,
315 Environmental change and atmospheric contamination on Svalbard: sediment chronology, P. G.
316 Appleby, with kind permission from Springer Science+Business Media B.S.
317
318 Figure 2. Decadal-scale resolution of Hg accumulation in sediments of Svalbard lakes,
319 expressed as a fraction of preindustrial (1800-1850) Hg accumulation. For Ossian Sarsfjellet
320 (C), the preindustrial Hg record is not reliable (because of a "slump" event; Appleby 2004), and
321 we instead used the value from the period 1910-1920 as the denominator in calculating ratios.
322 Results are not shown for Tendammen (U), which is affected by local pollution and has Hg
323 accumulation ratios of 10-20 in sediments deposited since 1970.
324
325 Figure 3. Simple linear regression of catchment-area-to-lake-area ratio and preindustrial (pre-
326 1850; gray symbols, line) and modern (1985-1995; black symbols, line) Hg accumulation rates
327 for sediments of lakes from Svalbard. According to the model of Swain et al. (1992), the
328 intercept represents net atmospheric Hg deposition to a lake with no catchment, yielding
329 estimates from our dataset of 2.5 and 7 $\mu g/m^2/y$ for preindustrial and modern periods,
330 respectively. Ossian Sarsfjellet (C) was not included in the preindustrial model because the
331 preindustrial Hg record in this lake is not reliable (because of a "slump" event; Appleby 2004).
332 Tendammen (U) was not included in the modern model because this lake is affected by local
333 pollution.

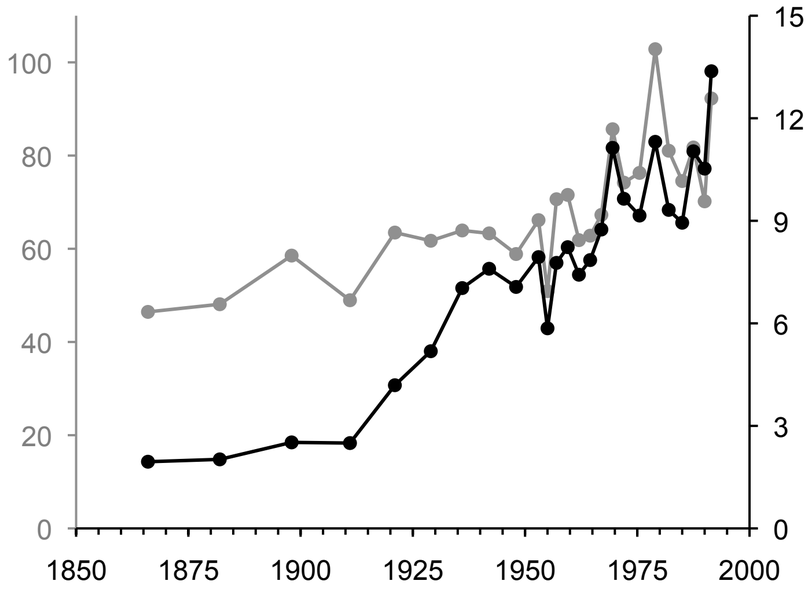
100
80
60
40
20
0
15
12
9
6
3
0
1850
1875
1900
1925
1950
1975
2000

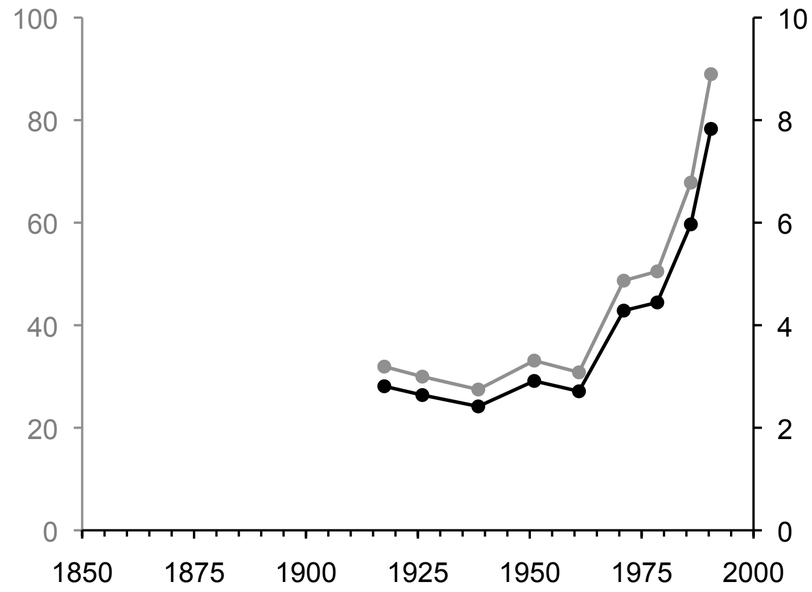
100
80
60
40
20
0
10
8
6
4
2
0
1850
1875
1900
1925
1950
1975
2000

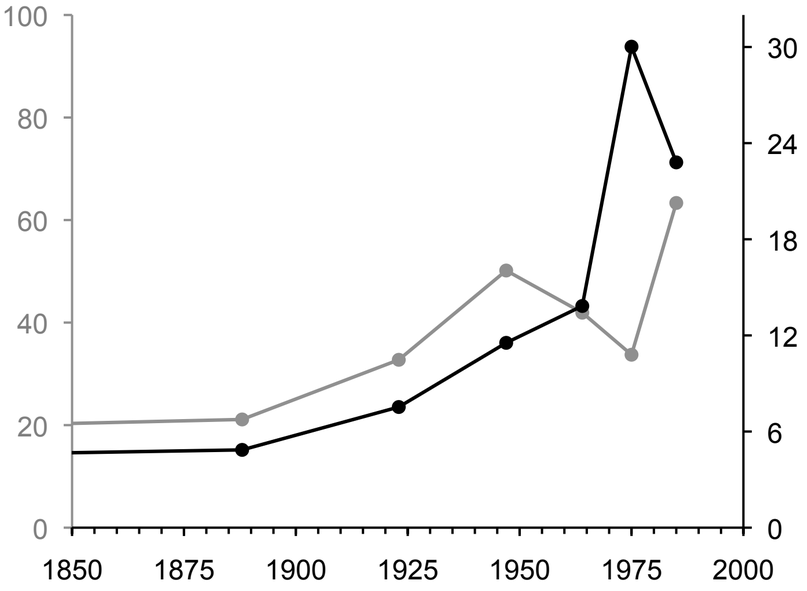
100
80
60
40
20
0
30
24
18
12
6
0
1850
1875
1900
1925
1950
1975
2000

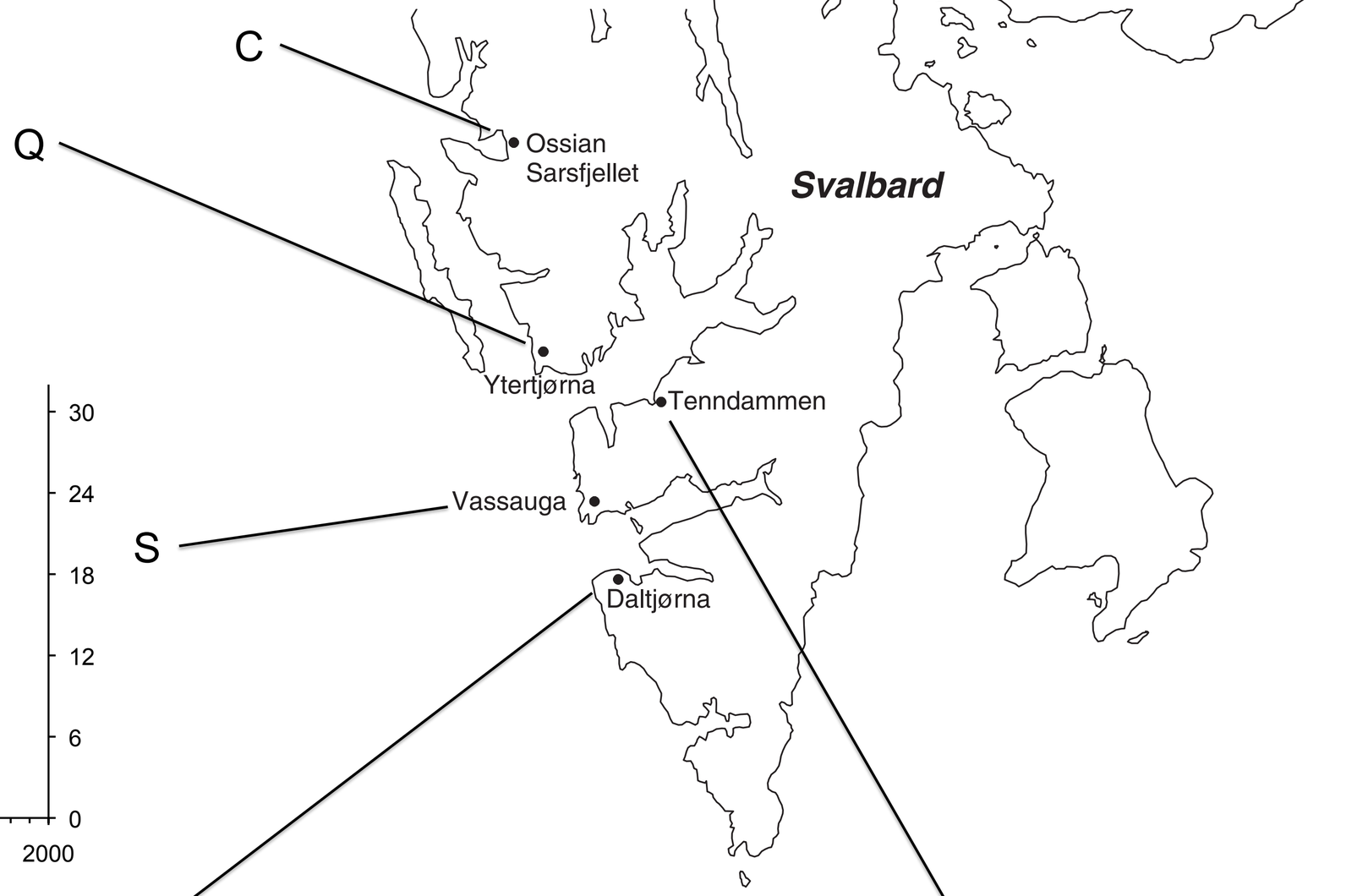
C
Q
S
T
U
Ossian
Sarsfjellet
Svalbard
Ytertjørna
Tenndammen
Vassauga
Daltjørna

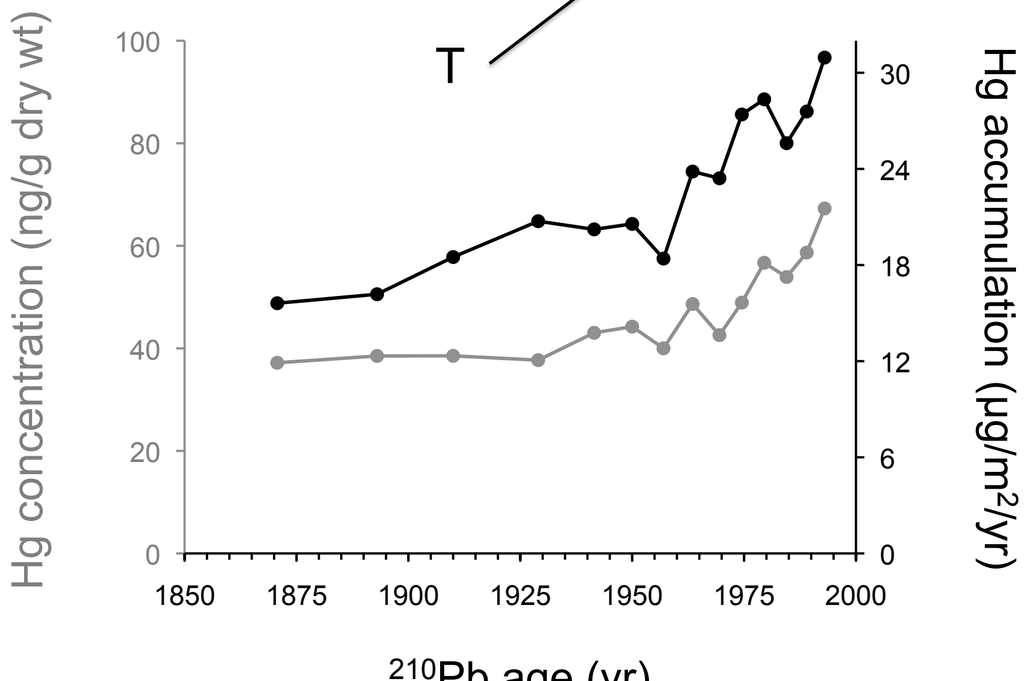
Hg concentration (ng/g dry wt)
Hg accumulation (µg/m²/yr)
100
80
60
40
20
0
30
24
18
12
6
0
1850
1875
1900
1925
1950
1975
2000
210Pb age (yr)

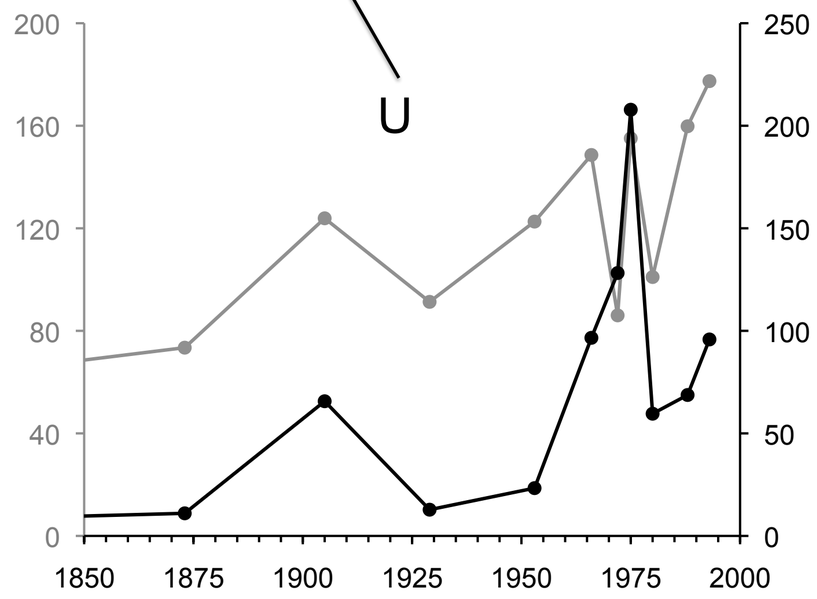
200
160
120
80
40
0
250
200
150
100
50
0
1850
1875
1900
1925
1950
1975
2000

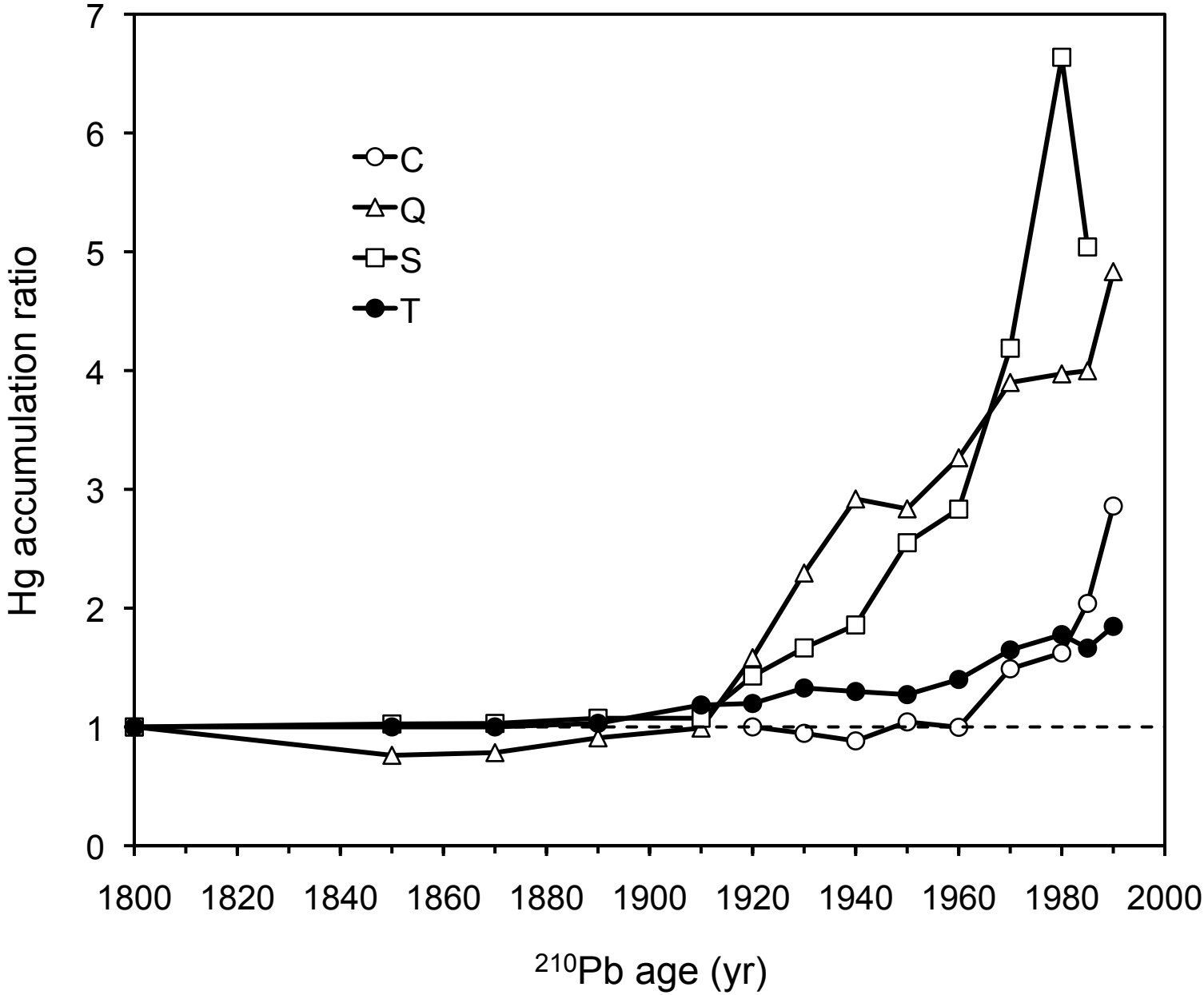
C
Q
S
T
Hg accumulation ratio
0
1
2
3
4
5
6
7
1800
1820
1840
1860
1880
1900
1920
1940
1960
1980
2000
210Pb age (yr)

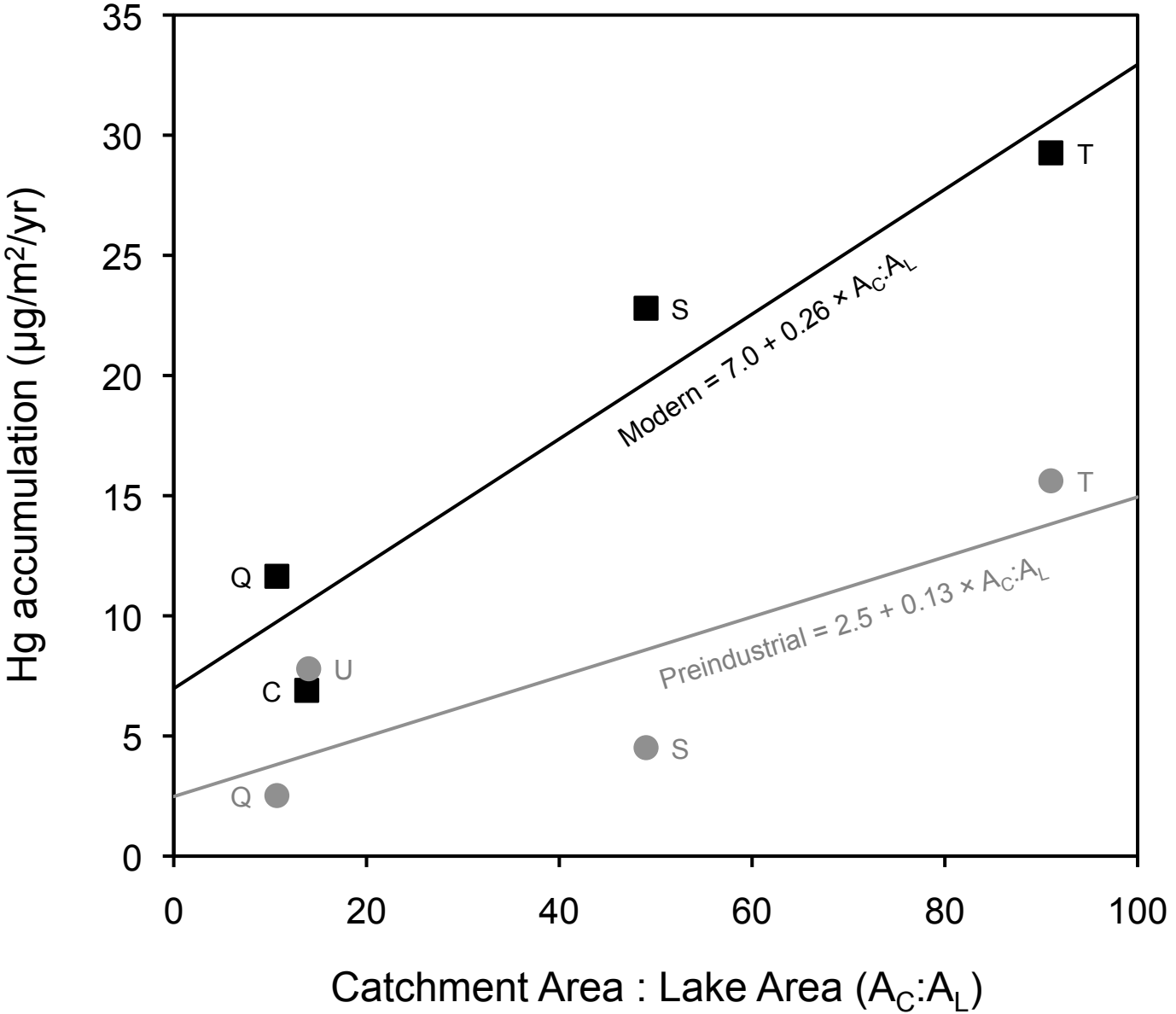
Hg accumulation (µg/m²/yr)
Catchment Area : Lake Area (A_C:A_L)
0
5
10
15
20
25
30
35
0
20
40
60
80
100
Modern = 7.0 + 0.26 × A_C:A_L
Preindustrial = 2.5 + 0.13 × A_C:A_L
T
S
Q
C
U
T
S
Q

Supplementary Data

Net Atmospheric Mercury Deposition to Svalbard: Estimates from Lacustrine Sediments

Paul E. Drevnick, Handong Yang, Carl H. Lamborg, and Neil L. Rose

Hg concentration and Hg accumulation in lake sediment cores.
^{210}Pb-based ages and sedimentation rates can be found in Appleby (2004).

lake	lake code	core	interval top (cm)	interval bottom (cm)	Hg conc. (ng/g dw)	Hg accum. (ug/m^2/yr)
Ossian Sarsfjellet	C	SBAC2	0	0.25	89	7.8
Ossian Sarsfjellet	C	SBAC2	0.25	0.5	68	6.0
Ossian Sarsfjellet	C	SBAC2	0.5	0.75	51	4.4
Ossian Sarsfjellet	C	SBAC2	0.75	1	49	4.3
Ossian Sarsfjellet	C	SBAC2	1	1.25	31	2.7
Ossian Sarsfjellet	C	SBAC2	1.25	1.5	33	2.9
Ossian Sarsfjellet	C	SBAC2	1.5	1.75	27	2.4
Ossian Sarsfjellet	C	SBAC2	1.75	2	30	2.6
Ossian Sarsfjellet	C	SBAC2	2	2.25	32	2.8
Yterjørna	Q	SBAQ1	0.5	0.75	92	13.4
Yterjørna	Q	SBAQ1	0.75	1	70	10.5
Yterjørna	Q	SBAQ1	1	1.25	82	11.0
Yterjørna	Q	SBAQ1	1.25	1.5	75	8.9
Yterjørna	Q	SBAQ1	1.5	1.75	81	9.3
Yterjørna	Q	SBAQ1	1.75	2	103	11.3
Yterjørna	Q	SBAQ1	2	2.25	76	9.2
Yterjørna	Q	SBAQ1	2.25	2.5	74	9.6
Yterjørna	Q	SBAQ1	2.5	2.75	86	11.1
Yterjørna	Q	SBAQ1	2.75	3	67	8.7
Yterjørna	Q	SBAQ1	3	3.25	63	7.9
Yterjørna	Q	SBAQ1	3.25	3.5	62	7.4
Yterjørna	Q	SBAQ1	3.5	3.75	72	8.2
Yterjørna	Q	SBAQ1	3.75	4	71	7.8
Yterjørna	Q	SBAQ1	4	4.25	51	5.9
Yterjørna	Q	SBAQ1	4.25	4.5	66	7.9
Yterjørna	Q	SBAQ1	4.75	5	59	7.1
Yterjørna	Q	SBAQ1	5	5.5	63	7.6
Yterjørna	Q	SBAQ1	5.5	6	64	7.0
Yterjørna	Q	SBAQ1	6	6.5	62	5.2
Yterjørna	Q	SBAQ1	6.5	7	63	4.2
Yterjørna	Q	SBAQ1	7	7.5	49	2.5
Yterjørna	Q	SBAQ1	7.5	8	59	2.5
Yterjørna	Q	SBAQ1	8	8.5	48	2.0

Yterjørna	Q	SBAQ1	8.5	9	46	2.0
Yterjørna	Q	SBAQ1	9	9.5	46	1.9
Yterjørna	Q	SBAQ1	9.5	10	61	2.6
Yterjørna	Q	SBAQ1	10.5	11	61	2.6
Yterjørna	Q	SBAQ1	11.5	12	51	2.1
Yterjørna	Q	SBAQ1	12.5	13	79	3.3
Yterjørna	Q	SBAQ1	13.5	14	68	2.8
Yterjørna	Q	SBAQ1	14.5	15	64	2.7
Yterjørna	Q	SBAQ1	15.5	16	61	2.6
Yterjørna	Q	SBAQ1	16.5	17	50	2.1
Yterjørna	Q	SBAQ1	17.5	18	55	2.3
Yterjørna	Q	SBAQ1	18.5	19	60	2.5
Yterjørna	Q	SBAQ1	19.5	20	64	2.7
Vassauga	S	SBAS3	1	2	63	22.8
Vassauga	S	SBAS3	2	3	34	30.0
Vassauga	S	SBAS3	3	4	42	13.8
Vassauga	S	SBAS3	4	5	50	11.5
Vassauga	S	SBAS3	5	6	33	7.5
Vassauga	S	SBAS3	6	7	21	4.9
Vassauga	S	SBAS3	7	8	20	4.6
Vassauga	S	SBAS3	8	9	11	2.6
Vassauga	S	SBAS3	9	10	20	4.6
Vassauga	S	SBAS3	10	11	25	5.7
Vassauga	S	SBAS3	11	12	16	3.7
Vassauga	S	SBAS3	12	13	16	3.6
Vassauga	S	SBAS3	13	14	23	5.3
Vassauga	S	SBAS3	14	15	25	5.8
Vassauga	S	SBAS3	15	16	20	4.7
Daltjørna	T	SBAT1	0	0.25	67	30.9
Daltjørna	T	SBAT1	0.5	0.75	59	27.6
Daltjørna	T	SBAT1	1	1.25	54	25.6
Daltjørna	T	SBAT1	1.5	1.75	57	28.3
Daltjørna	T	SBAT1	2	2.25	49	27.4
Daltjørna	T	SBAT1	2.5	2.75	43	23.4
Daltjørna	T	SBAT1	3	3.25	49	23.8
Daltjørna	T	SBAT1	3.5	3.75	40	18.4
Daltjørna	T	SBAT1	4	4.25	44	20.6
Daltjørna	T	SBAT1	4.5	4.75	43	20.2
Daltjørna	T	SBAT1	5	5.5	38	20.7
Daltjørna	T	SBAT1	6	6.5	39	18.5
Daltjørna	T	SBAT1	7	7.5	39	16.2
Daltjørna	T	SBAT1	8	8.5	37	15.6
Tenndammen	U	SBAU4	0	1	177	95.8

Tenndammen	U	SBAU4	1	2	160	68.7
Tenndammen	U	SBAU4	2	3	101	59.6
Tenndammen	U	SBAU4	3	4	155	207.8
Tenndammen	U	SBAU4	4	5	86	128.2
Tenndammen	U	SBAU4	5	6	149	96.6
Tenndammen	U	SBAU4	6	7	123	23.3
Tenndammen	U	SBAU4	7	8	91	12.8
Tenndammen	U	SBAU4	8	9	124	65.7
Tenndammen	U	SBAU4	9	10	73	11.0
Tenndammen	U	SBAU4	10	11	59	7.1
Tenndammen	U	SBAU4	12	13	67	8.0
Tenndammen	U	SBAU4	13	14	67	8.0
Tenndammen	U	SBAU4	14	15	68	8.2
Tenndammen	U	SBAU4	15	16	60	7.2
Tenndammen	U	SBAU4	16	17	51	6.1
Tenndammen	U	SBAU4	17	18	83	10.0